13

Trajectory analysis in a collector with multistage energy recovery for a DEMO prototype gyrotron. Part III. Influence of the spent electron beam parameters

© O.I. Louksha,[1] A.S. Zuev,[2] A.G. Malkin,[1] E.S. Semenov,[2] P.A. Trofimov,[1] M.Yu. Glyavin[2]

[1]Peter the Great Saint-Petersburg Polytechnic University, St. Petersburg, Russia
[2]Institute of Applied Physics, Russian Academy of Sciences, Nizhny Novgorod, Russia
e-mail: louksha@rphf.spbstu.ru

Received January 31, 2023
Revised March 3, 2023
Accepted March 11, 2023

The influence of the spent electron beam parameters on the possibilities of multistage energy recovery in the prototype gyrotron developed for the DEMO project is determined. The characteristics of electrodes and magnetic coils in a collector with four-stage recovery were optimized considering the distributions of electrons' coordinates and velocities obtained as a result of calculating the electron-wave interaction in the cavity. In the trajectory analysis in the collector, a sectioned electron beam was used to suppress the negative influence of the bundles of a toroidal solenoid used to create an azimuthal magnetic field. The possibility of achieving the total efficiency of the gyrotron of approximately 78% was shown, which is close to the maximum total efficiency with ideal separation of electron fractions with different energies, with the current of electrons reflected from the collector not exceeding 1% of the total current of the electron beam.

Keywords: Microwave electronics, gyrotron, electron beam, energy recovery.

DOI: 10.21883/TP.2023.05.56075.14-23

Introduction

Recovery of the residual energy of the spent electron beam — is a widely used method for increasing the efficiency of vacuum sources of microwave radiation (see, for example, [1]). In collectors with recovery, electrons are inhibited in an electric field, thus returning to the electrical network part of their energy, unspent during their interaction with the electromagnetic field in the electrodynamic structure. The vast majority of today's gyrotrons, the most powerful radiation sources in the millimeter and submillimeter wavelength ranges, use collectors with single-stage recovery. For example, single-stage recovery allows increasing the total efficiency up to 50−55% in megawatt-level gyrotrons designed for plasma heating and current control in controlled fusion plants [2–5], and even up to 60% in gyrotrons designed for microwave technologies [6]. In order to achieve even higher efficiency and additional reduction of the thermal load on the collector, it is desirable to make a transition to systems with multi-stage recovery of residual electron energy, for which it is necessary to ensure spatial separation of electron fractions with different energies and deposition of these fractions on the collector sections under different braking potentials. The electrons in helical electron beam (HEB) of gyrotrons can be spatially separated as a result of their drift in crossed electric and magnetic fields [7–10]. Peter the Great St. Petersburg Polytechnic University (SPbPU) conducts studies for determining the possibilities of effective separation of electrons in longitudinal electric and azimuthal magnetic fields and the development on this basis of collectors with multi-stage recovery for gyrotrons (for example, [11,12]). In particular, a collector system for the SPbPU gyrotron with a frequency of 74.2GHz and an output power of approximately 100 kW [13,14], in which a solenoid with a toroidal winding is used to create an azimuthal magnetic field.

At the previous stages of [15,16], calculations of a collector with four-stage recovery were performed for a prototype gyrotron with a frequency of 250GHz, being developed for the DEMO project [17,18]. The study determined the distributions of electric and magnetic fields in the collector region at which effective separation of electrons of the processed HEB is achieved with a small reflection of electrons from the collector towards the resonator. Both a variant with an idealized distribution of the azimuthal magnetic field [15], which was created by a conductor located on the axis of the device, and a system with an azimuthal magnetic field created by a toroidal solenoid [16] are analyzed. In both cases, the characteristics of the particles at the collector inlet were set „manually" using the typical electron energy spectrum in the processed HEB, determined for high-power gyrotrons based on experimental data.

This article, which is a continuation of the work [15,16], provides the results of modeling of the collector for the prototype of the DEMO gyrotron which were obtained using the analysis of electron-wave interaction in the resonator of this gyrotron within the framework of a self-consistent model implemented in the ANGEL [19,20] software which allowed for determining the characteristics of the processed

HEB. All calculations in the collector area were performed using 3*D*-modeling software CST Studio Suite [21].

1. Gyrotron operating regime and electron beam parameters

The current version of the gyrotron prototype for the DEMO project, developed in the Institute of Applied Physics of the Russian Academy of Sciences, is characterized by the following main parameters: magnetic field induction in the resonator $B_0 \approx 9.5\,\mathrm{T}$, accelerating voltage $U_0 = 55\,\mathrm{kV}$, beam current $I_\mathrm{b} = 20\,\mathrm{A}$. To determine the array of data on particle parameters in the output plane of the resonator $z = 90\,\mathrm{mm}$ ($z = 0$ corresponds to the central plane of the resonator) (1) trajectory analysis in the region of formation and transportation of HEB to the specified output plane and (2) self-consistent calculation of electron-wave interaction in a resonator based on averaged equations were performed. Such calculations are described, for example, in the papers [19,20,22].

The trajectory analysis was performed taking into account the initial velocity spread of electrons for homogeneous and sectioned azimuthal distributions of the emission current from the cathode thermal belt. The number of emission centers was chosen to be 600 for homogeneous and 1176 for sectioned distributions. The spread of the initial velocities was set to 5.9% [1] with a Gaussian velocity distribution function. The number of beam fractions with different velocities was 13. In the case of a sectioned distribution, there was no electron emission in two symmetrically arranged azimuthal cathode sectors with a length of 45° each. The sectioning of the HEB allows reducing the negative impact of the magnetic field of the bundles of the toroidal solenoid used to create an azimuthal magnetic field in the recovery area [16]. The values of the transverse velocity spread in the beam entering the resonator obtained as a result of trajectory analysis were equal to 13.4% for homogeneous and 20.2% for sectioned distributions.

When modeling the electron-wave interaction, 57 HEB fractions with different values of transverse velocity were fed into the resonator. Each HEB fraction consisted of 17 fractions differing in the phase of entry into the working region. The values of the transverse velocity were set according to the velocity spectrum determined at the stage of trajectory analysis in an electron-optical system. The parameters of the output radiation of the gyrotron and the characteristics of the spent HEB were calculated taking into account the inhomogeneous magnetic field of the cryosolenoid, ohmic losses in the resonator and the beam potential depression. The power of the microwave radiation P_out was 374.9 kW for homogeneous and 363.3 kW for sectioned distributions of the emission current. At the same time, approximately 8% of the power P_el taken from the electron beam in the resonator was spent on heating its wall. The electronic efficiency η_el was determined using the ratio

$$\eta_\mathrm{el} = \frac{P_\mathrm{el}}{I_\mathrm{b}(U_0 - \Delta U)},$$

taking into account the beam potential depression ΔU. The values of these parameters for a homogeneous distribution are: $P_\mathrm{el} = 406.6\,\mathrm{kW}$, $\Delta U = 3.65\,\mathrm{kV}$, $\eta_\mathrm{el} = 39.6\%$, for a sectioned distribution: $P_\mathrm{el} = 394.4\,\mathrm{kW}$, $\Delta U = 3.94\,\mathrm{kV}$, $\eta_\mathrm{el} = 38.6\%$. The sectioning of the HEB, judging by the data obtained, led only to a slight drop in output power and electronic efficiency.

Data arrays containing information about coordinates, velocities and currents in the plane $z = 90\,\mathrm{mm}$, were obtained for $530 \cdot 10^3$ particles with homogeneous and for $1039 \cdot 10^3$ particles with sectioned emission distributions from the cathode. The electron energy spectra are shown in Fig. 1. A simplified spectrum used earlier in [15,16] is shown here in addition to the spectra for homogeneous and sectioned HEB. The fundamental difference between the spectra for real HEB compared to the simplified one is the presence of particles with large energy values exceeding the energy of $eU_0 = 55\,\mathrm{keV}$. At the same time, the spectrum width for a sectioned HEB is about twice as large as the spectrum width of a homogeneous HEB. New data on the characteristics of the spent electron beam obtained after calculations of the interaction of electrons with the electromagnetic field in the resonator required changes in the design and operating regimes of the collector to achieve maximum efficiency of recovery of residual electron energy. When modeling the collector, the input plane in which the particle sources were located was the plane $z = 430\,\mathrm{mm}$. To obtain the input interface, calculations of particle trajectories in the magnetic field generated generated by the main coil of gyrotron were performed in the region between $z = 90$ and 430 mm. Trajectory analysis in the collector region (see sec. 3) was performed only for a sectioned HEB in which the number of particles (current tubes) was reduced to about $25 \cdot 10^3$.

2. Optimization of magnetic field distribution in the collector region

The main elements of the upgraded collector for the DEMO gyrotron (Fig. 2) are similar to those described in [16]. It is important that the dimensions of this collector (length and radius of the cylindrical part) do not differ significantly from the corresponding dimensions of the collector without recovery [17,18]. There are sections S1−S4 under negative potentials used for electron deceleration in the cylindrical part of the collector body *1* with an internal radius of 160 mm. Correcting coils C1−C7 in combination with the main gyrotron magnetic system provide the required distribution of the longitudinal magnetic field. Solenoid with toroidal winding *2* is used to create an azimuthal magnetic field. The end conductors of this solenoid from the side closest to the resonator

[1] The values of the velocity spread given in this paper were determined as the standard deviation from the average velocity value.

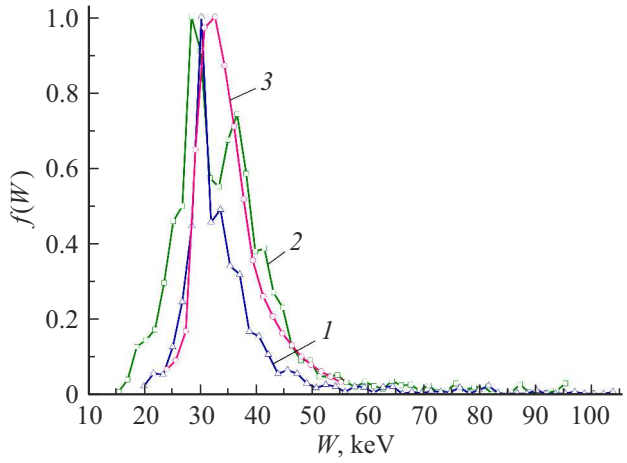

Figure 1. Electron energy distributions in the spent gyrotron beam: *1* — homogeneous HEB, *2* — sectioned HEB, *3* — simplified distribution used in the works [14,15].

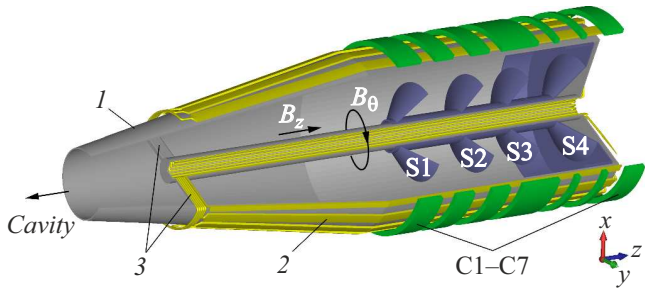

Figure 2. Schematic representation of the collector area of the gyrotron: *1* — collector body, *2* — toroidal solenoid, *3* — bundles, S1–S4 — collector sections, C1–C7 — correcting coils.

are assembled into two radial bundles *3* located in the connecting tubes.

The distribution of the magnetic field was optimized based on the results of the calculation of the trajectories of „single“ electrons. Point sources of particles were set in the plane $z = 430$ mm. The initial energy and radial coordinate of all particles were the same and were equal to 36 keV and 27 mm, respectively, and the azimuthal coordinate θ was different. Fig. 3 shows projections of electron trajectories on the plane $r-z$ for different coordinate values θ in the range from 0° to 180° (Fig. 3, *a*) and the distribution of the various components of the magnetic field induction along the longitudinal coordinate z (Fig. 3, *b*). Due to the symmetry of the system, the electron trajectories for θ in the range from 180° to 360° will coincide with those shown in Fig. 3, *a*. This figure also shows the relative position of the emission points and the bundles of the toroidal solenoid. The azimuthal position of the bundles corresponding to the coordinates $\theta = 115°$ and 295°, in turn, was chosen taking into account the position of the HEB sectors in which there are no electrons (see below). Particles with high energies present in the spectrum of the spent HEB (Fig. 1) can acquire a significant transverse velocity in the region of the bundles of the toroidal solenoid. Moving along trajectories with large Larmor radii, these electrons can settle on the collector walls without reaching sections with potentials corresponding to their energy. The average beam radius in the recovery area was reduced ($z > 1000$ mm) for reduction of the current to the collector body, by increasing the induction of the longitudinal magnetic field compared to the collector described in [16]. The induction of the longitudinal magnetic field B_z in this region was approximately 0.02 T, and the azimuthal field B_θ — approximately 0.032 T (Fig. 3, *b*). These values were determined on the average beam radius $r = 110$ mm.

For the efficient operation of recuperation it is important to ensure a minimum spread of the radial position of the electron trajectories with different values of the azimuthal coordinate of the point of entry into the collector in the absence of voltage on the sections. As the previous calculations of [16] have shown, this can be achieved by choosing the positive direction of the azimuthal magnetic field (Fig. 2 and 3), as well as by selecting the required field value of the main gyrotron magnetic system and correcting coils in the area of the toroidal solenoid bundles

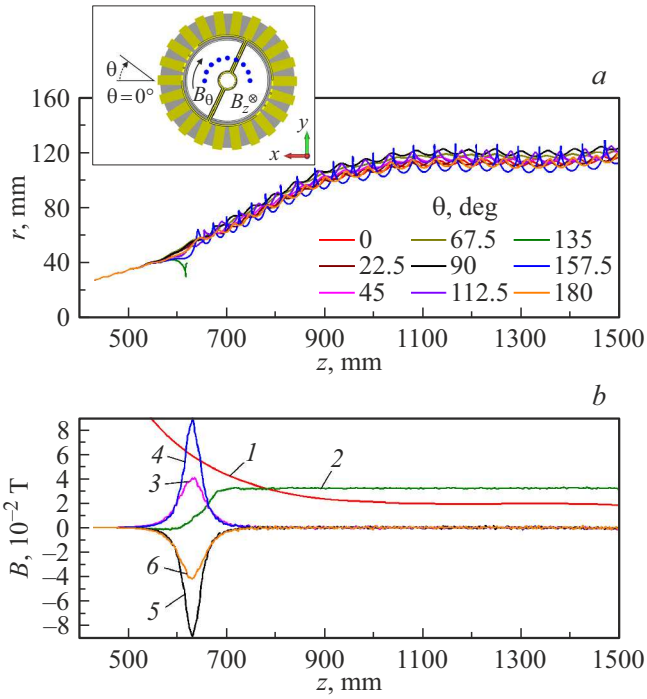

Figure 3. *a* — projections of trajectories of „single“ electrons with different azimuthal coordinates of the starting point θ; *b* — distribution of magnetic field induction determined at different values of coordinates r and θ along the coordinate z for the field of the main magnetic system of the gyrotron and correcting coils at $r = 110$ mm, $\theta = 0°$ (*1*), azimuthal field of toroidal solenoid at $r = 110$ mm, $\theta = 0°$ (*2*), longitudinal field of toroidal solenoid at $r = 50$ mm and $\theta = 72.5°$ (*3*), 95° (*4*), 135° (*5*), 157.5° (*6*). The insertion shows the azimuthal position of the emission points of „single“ electrons and bundles of a toroidal solenoid.

($z \approx 630$ mm) to compensate for the parasitic effect of the longitudinal component of the field of this solenoid (Fig. 3, *b*). It can be seen (Fig. 3, *a*) that with the optimized distribution of the magnetic field, there is no noticeable variation in the radial position of the electronic trajectories in the recovery region.

However, after the optimization, there are still electrons moving in close proximity to the bundles of the toroidal solenoid, whose trajectories are noticeably curved under the influence of the parasitic field of this solenoid. Such electrons may not reach the section with a potential corresponding to their energy, but settle on other electrodes of the collector, or are reflected from the collector towards the resonator. In both cases, the efficiency of the recuperator decreases. For example, an electron with the initial coordinate $\theta = 135°$ settles on the connecting tube in which the bundle is located (Fig. 3, *a*). It can be seen that at the azimuth $\theta = 135°$ the total longitudinal field, which is determined by the sum of the values B on the curves *1* and *5*, changes its direction from positive to negative and back when moving along the axis z (fig. 3, *b*). The sectioning of the HEB was performed as described in section 1 to eliminate the negative impact of such electrons on the operation of the recuperator.

3. Trajectory analysis in a collector with four-stage recovery

For the spectrum of the spent HEB (Fig. 1), in which 1000 energy fractions were allocated, the maximum total efficiency during four-stage recovery with ideal separation, when each energy fraction from the spectrum of the spent HEB falls on the section at a potential corresponding to its energy [8,12], was 80.3%. This value was obtained

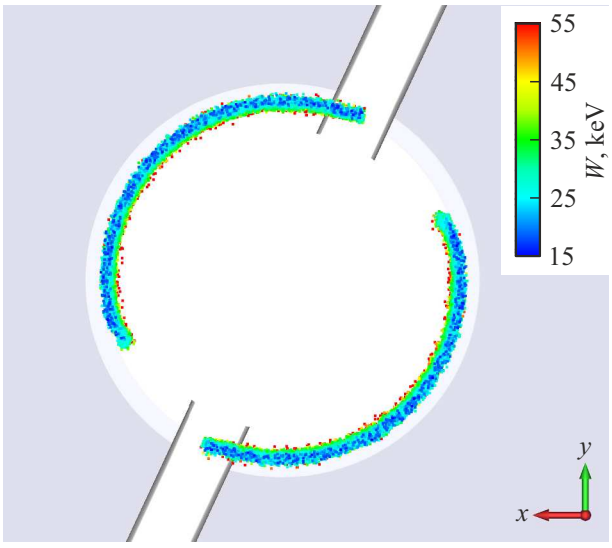

Figure 4. Particle distribution in the plane $x-y$ ($z = 430$ mm) for a sectioned HEB. The color corresponds to the energy of the particles W.

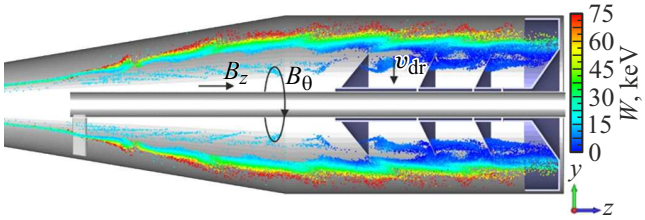

Figure 5. The position of the particles in the plane $y-z$ ($x = 0$). The color corresponds to the energy of the particles W.

by iterating over the values of $U_{S1}-U_{S4}$ with a step of 0.2 kV, provided that 1% of the HEB current with electrons having the lowest energy is reflected from the collector. For comparison, the values of the maximum total efficiency with a different number of recovery stages N are equal to: 68.8% (N=2), 76.8% ($N = 3$), 82.9% ($N = 5$), 85.0% ($N = 6$). As in previous studies [11,12,15,16], the choice of the number of stages equal to four is the result of a compromise between the desire to achieve the maximum total efficiency of the gyrotron and the difficulties of practical implementation of a recovery system with a large number of stages.

Four cone-shaped sections under braking potentials were located in the recovery area (Fig. 2). The radii of the bases of these sections were reduced compared to those described in [16] due to a decrease in the average beam radius. The results of calculations of the total efficiency of the gyrotron with ideal separation were used to select the potentials of the sections $U_{S1}-U_{S4}$.

The position of the particles of the spent HEB in the inlet plane of the collector is shown in Fig. 4. There is a displacement of electrons in the radial direction in the areas adjacent to the cut out HEB sectors, under the action of the crossed azimuthal electric field of the spatial charge and the longitudinal magnetic field (the diocotron effect). The length of the sectors in this plane is approximately 40°. Their azimuthal position ($117° < \theta < 157°$ and $297° < \theta < 337°$) relative to the bundles of the toroidal solenoid was optimized to achieve minimal reflection of electrons from the collector.

A minor correction of the potentials $U_{S1}-U_{S4}$ obtained with ideal separation was performed to achieve the maximum total efficiency of the gyrotron as a result of a series of calculations of electron trajectories in the collector. At $U_{S1} = -18.8$ kV, $U_{S2} = -27.4$ kV, $U_{S3} = -34.3$ kV, $U_{S4} = -40.7$ kV (collector body potential $U_{coll} = 0$) the power dissipated on sections and body, respectively, were $P_{S1} = 22.7$ kW, $P_{S2} = 27.3$ kW, $P_{S3} = 16.4$ kW, $P_{S4} = 39.9$ kW, $P_{coll} = 1.2$ kW with a reflection coefficient from the collector of 0.99 %. The total power P_{diss} dissipated on the collector is thus equal to 107.5 kW. At power $P_{el} = 394.4$ kW the total efficiency of the gyrotron

$$\eta_t = \frac{P_{el}}{P_{el} + P_{diss}} = 78.6\%,$$

and the collector efficiency (recovery efficiency) $\eta_{\text{oll}} = 84.8\%$. Here, when calculating the total efficiency, as in the previous calculations of [15,16], power losses associated with heating the walls of the resonator were not taken into account.

Thus, the optimization of the geometry of collector sections geometry and field distributions made it possible to obtain a value of the total efficiency of the gyrotron only slightly less than the maximum efficiency in a four-stage recovery system with ideal electron separation. Taking into account the real distribution of electrons by coordinates and velocities in the spent HEB led to a decrease in efficiency by about 5% compared to the value obtained in the work [16] with a simplified method of setting the parameters of the HEB.

Figure 5 shows the position of particles in the plane $y-z$, obtained as a result of the intersection of helical electronic trajectories with this plane. It can be seen that, moving in a retarding electric field in the recovery region, the electrons are displaced by the action of crossed E_z and B_θ fields in the radial direction, in this case towards smaller radii with the selected field direction B_θ. Most of the electrons are deposited on the back walls of the sections after changing the direction of their longitudinal movement. With an increase in the initial energy of the electrons, they travel a greater distance along the axis z and are deposited on sections with a more negative potential.

The calculated thermal load distribution over the surfaces of the collector sections was similar to that described in [16]. The maximum power density at the same time was approximately 0.3 kW /cm^2, which is acceptable for the operation of the gyrotron in quasi-continuous regime. A further increase in the HEB power and the transition to a megawatt level of microwave output power will obviously require additional refinement of the collector design, taking into account intensive water cooling.

Conclusion

Thus, the study, divided into three parts, was aimed at determining the possibilities of implementing multi-stage energy recovery of the spent electron beam in the gyrotron, which was developed as a prototype for the DEMO gyrotron. In the first part [15], the prospects of the method of spatial separation of electronic fractions with different energies in crossed longitudinal electric and azimuthal magnetic fields are shown, which can be used to implement multi-stage recovery. The conditions of effective recovery are determined in the second part [16] for using a solenoid with toroidal winding as a source of azimuthal magnetic field. In this paper, the geometry of the electrodes and magnetic coils in the collector region of the gyrotron was refined, taking into account the real distribution of electrons in coordinates and velocities in the spent HEB, obtained as a result of calculations of the electron-wave interaction in the resonator.

The main limitation in the implementation of the proposed recuperator design is the presence of end conductors of a toroidal solenoid, which are located on the side closest to the resonator. These conductors are assembled in two bundles to increase the passage of electrons to the recovery area. The negative impact of the magnetic field of these bundles on the recovery efficiency and the electron reflection coefficient from the collector is reduced due the sectioning of the electron beam.

It is shown that in the developed collector with four-stage recovery, a total efficiency value of approximately 78% can be achieved for a gyrotron with real HEB, which is close to the maximum efficiency with ideal separation of electron beam fractions with different energies. This efficiency value was obtained for a gyrotron with a sectioned cathode containing two sectors with a length of 45° from which there is no electron emission. The sectioning of the HEB made it possible, in particular, to reduce the electron reflection coefficient from the collector to about 1%. A further improvement of the azimuthal magnetic field source may become a continuation of this work which will simplify the design of the collector.

Acknowledgments

The authors are grateful to V.E. Zapevalov for valuable comments and interest in the work.

Funding

The study was supported by a grant from the Russian Science Foundation (Project № 22-29-00136). Some of the results were obtained using the computing resources of the supercomputing center of Peter the Great St. Petersburg Polytechnic University (http://www.scc.spbstu.ru).

Conflict of interest

The authors declare that they have no conflict of interest.

References

[1] H.G. Kosmahl. Proc. IEEE, **70** (11), 1325 (1982). DOI: 10.1109/PROC.1982.12481
[2] K. Sakamoto, M. Tsuneoka, A. Kasugai, T. Imai, T. Kariya, K. Hayashi, Y. Mitsunaka. Phys. Rev. Lett., **73** (26), 3532 (1994). DOI: 10.1103/PhysRevLett.73.3532
[3] M.Y. Glyavin, A.N. Kuftin, N.P. Venediktov, V.E. Zapevalov. Int. J. Infrared Millimeter Waves, **18**, 2129 (1997). DOI: 10.1007/BF02678255
[4] M. Thumm. J. Infrared Millimeter Terahertz Waves, **41** (1), 1 (2020). DOI: 10.1007/s10762-019-00631-y
[5] V.N. Manuilov, M.V. Morozkin, O.I. Luksha, M.Y. Glyavin. Infrared Physics and Technology, **91**, 46 (2018). DOI: 10.1016/j.infrared.2018.03.024
[6] M.V. Morozkin, M.Y. Glyavin, G.G. Denisov, A.G. Luchinin. Int. J. Infrared Millimeter Waves, **29** (11), 1004 (2008). DOI: 10.1007/s10762-008-9408-z

[7] I.Gr. Pagonakis, J.P. Hogge, S. Alberti, K.A. Avramides, J.L. Vomvoridis. IEEE Trans. Plasma Sci., **36** (2), 469 (2008). DOI: 10.1109/TPS.2008.917943
[8] O.I. Louksha, P.A. Trofimov. Tech. Phys. Lett., **41** (9), 884 (2015). DOI: 10.1134/S1063785015090230
[9] C. Wu, I.G. Pagonakis, K.A. Avramidis, G. Gantenbein, S. Illy, M. Thumm, J. Jelonnek. Phys. Plasmas, **25** (3), 033108 (2018). DOI: 10.1063/1.5016296
[10] B. Ell, C. Wu, G. Gantenbein, S. Illy, M. Misko, I.G. Pagonakis, J. Weggen, M. Thumm, J. Jelonnek. IEEE Trans. Electron Devices, **70** (3), 1299 (2023). DOI: 10.1109/TED.2023.3234885
[11] O.I. Louksha, P.A. Trofimov. *Proc. 18th Int. Vacuum Electronics Conf., IVEC 2017* (London, United Kingdom, 2017), p. 1. DOI: 10.1109/IVEC.2017.8289518
[12] O.I. Louksha, P.A. Trofimov. Tech. Phys., **64** (12), 1889 (2019). DOI: 10.1134/S1063784219120156
[13] D.V. Kas'yanenko, O.I. Louksha, B. Piosczyk, G.G. Sominsky, M. Thumm. Radiophys. Quantum Electron, **47** (5–6), 414 (2004). DOI: 10.1023/B:RAQE.0000046315.10190.1c
[14] O. Louksha, B. Piosczyk, G. Sominski, M. Thumm, D. Samsonov. IEEE Trans. Plasma Sci., **34** (3), 502 (2006). DOI: 10.1109/TPS.2006.875779
[15] O.I. Louksha, P.A. Trofimov, V.N. Manuilov, M. Yu. Glyavin. Tech. Phys., **66** (1), 118 (2021). DOI: 10.1134/S1063784221010138
[16] O. I. Louksha, P. A. Trofimov, V. N. Manuilov, M. Yu. Glyavin. Tech. Phys., **66** (8), 992 (2021). DOI: 10.1134/S1063784221070082
[17] M. Glyavin, V. Manuilov, M. Morozkin. *Proc. 43rd Int. Conf. Infrared, Millimeter, and Terahertz Waves* (Nagoya, Japan, 2018), 8510139.
[18] G.G. Denisov, M.Yu. Glyavin, A.P. Fokin, A.N. Kuftin, A.I. Tsvetkov, A.S. Sedov, E.A. Soluyanova, M.I. Bakulin, E.V. Sokolov, E.M. Tai, M.V. Morozkin, M.D. Proyavin, V.E. Zapevalov. Rev. Scientific Instrum., **89** (8), 084702 (2018). DOI: 10.1063/1.5040242
[19] E.S. Semenov, O.P. Plankin, R.M. Rosenthal. Izvestiya VUZ Applied Nonlinear Dynamics., **23** (3), 94 (2015) (in Russian). DOI: 10.18500/0869-6632-2015-23-3-94-105
[20] E.S. Semenov, A.S. Zuev, A.P. Fokin. Information and mathematical technologies in science and management, **1** (25), 35 (2022). DOI: 10.38028/ESI.2022.25.1.003
[21] CST Studio Suite. *Electromagnetic Field Simulation Software* [Electronic source] Available at: https://www.3ds.com/products-services/simulia/products/cst-studio-suite/
[22] N.A. Zavol'sky, V.E. Zapevalov, M.A. Moiseev. Radiophys. Quantum Electron., 64 (3), 175 (2021). DOI: 10.1007/s11141-021-10121-8

Translated by A.Akhtyamov